Journal of Materials Chemistry A

PAPER

View Article Online
View Journal | View Issue

Cite this: J. Mater. Chem. A, 2014, 2, 20083

Polytriphenylamine derivative with high free radical density as the novel organic cathode for lithium ion batteries

Chang Su,[a] Fang Yang,[b] Lvlv Ji,[b] Lihuan Xu*[a] and Cheng Zhang*[b]

Received 4th July 2014
Accepted 18th August 2014

DOI: 10.1039/c4ta03413a

www.rsc.org/MaterialsA

Polytriphenylamine derivative, poly[*N*,*N*,*N*,*N*-tetraphenylphenylenediamine] (PDDP), with a high free radical density, has been synthesized and studied as a cathode material for organic free radical batteries for the first time. The chemical structure, morphology, and electrochemical properties of the prepared polymers were characterized by Raman spectra (RS), electron spin resonance (ESR), ultraviolet visible spectroscopy (UV-Vis), scanning electron microscopy (SEM), cyclic voltammograms (CV), and electrochemical impedance spectra (EIS), respectively. In addition, the charge–discharge properties of the prepared polymers were studied by galvanostatic charge–discharge testing. Compared to polytriphenylamine (PTPA), the fabricated lithium ion half-cells based on PDDP as the cathode exhibited two well-defined plateaus at two discharge voltages of 3.8 and 3.3 V *vs.* Li/Li^+ and an improved capacity of 129.1 mA h g^{-1}, which was very close to its theoretical capacity (130 mA h g^{-1}). The excellent electrochemical performances of the PDDP electrode were due to its stable chemical structure and high free radical density, which makes the PDDP a promising free radical cathode material for organic lithium secondary batteries.

1. Introduction

In today's modern society, growing public demand for use electric devices such as electric vehicles (EVs), laptop computers, and cell phones make it necessary for the fabrication of new secondary batteries with improved properties. Compared with the anode materials, it is a challenge to design high capacity, low-cost, and environmentally benign cathode materials.[1] For traditional inorganic transition metal oxide-based cathode materials (*e.g.*, $LiCoO_2$), the environmental requirements, toxicity, recycling, limited capacity, and disposal of battery components are becoming hot issues, which hinder their large scale applications for upcoming portable electronic devices.[2–4] As an alternative, organic compounds have been investigated as novel energy storage materials for the positive-electrode of lithium batteries, mainly organic conductive polymers (polyaniline, polythiophene, and polyimide),[5,6] organo-sulfur compounds,[7] carbonyl-based compounds,[8–11] and stable radical polymers,[12,13] *etc.*

Recently, stable radical polymers are emerging as promising candidates for organic cathode materials. Among these, polytriphenylamine (PTPA) and its derivatives have been studied intensively, due to their interesting physical properties, including excellent charge transport, electroluminescence, and thermal and morphological stabilities.[14] Moreover, PTPA containing repeat triphenylamine radical units belongs to the family of radical polymer in which a reversible radical redox process has been demonstrated to occur during charge and discharge processes.[15] Consequently, triphenylamine-based polymer materials have been explored recently as electrode materials for energy storage in applications such as super capacitors and lithium ion batteries.[16,17] As reported,[18] PTPA electrodes show good electrochemical performances and well-defined voltage plateaus (~3.6 V) as the cathode of lithium ion batteries, which could contribute to the reversible redox radicals nature of PTPA. However, the theoretical capacity of PTPA is currently only 109 mA h g^{-1}, which is lower than that of the currently used $LiCoO_2$ (about 140 mA h g^{-1}), therefore, limiting its further research as the desired cathode of high energy batteries with high energy density. As a solution to this, it would be an effective strategy to improve either the theoretical capacity (C) or the discharge voltage of PTPA (V), *i.e.*, by a molecular structure design strategy, to achieve high energy density batteries (Energy density $= C \times V$).

Poly[*N*,*N*,*N*,*N*-tetraphenylphenylenediamine] (PDDP) has a similar triphenylamine structure, but has a higher free radical density than PTPA, due to the increased number of radicals per repeating unit, which give it a higher theoretical specific capacity of 130 mA h g^{-1} and which enables its use as a potential electrode material with multi-electron reactions. Although even this type of polymer still has some

[a]College of Chemical Engineering, Shenyang University of Chemical Technology, Shenyang, 110142, P. R. China. E-mail: xulihuanss@163.com; Tel: +86-24-89383902
[b]State Key Laboratory Breeding Base of Green Chemistry Synthesis Technology, International Science and Technology Cooperation Base of Energy Materials and Application, College of Chemical Engineering and Materials Science, Zhejiang University of Technology, Hangzhou, 310014, P. R. China. E-mail: czhang@zjut.edu.cn

disadvantages, such as energy/power density, expensive catalyst need for the synthesis, long-term cyclability, and solubility of the organic radical polymers in electrolyte, and so on. Recent studies have demonstrated that PDDP and its derivatives generally show excellent charge transport and electroluminescence, and have been widely applied as organic electroluminescence (EL) materials, photo-conduction materials, and organic solar cells materials.[19] However, to the best of our knowledge, there are no relative reports for the application of PDDP as an electroactive material in lithium ion batteries. Herein, a novel strategy has been first explored to obtain a high performance, triphenylamine free, radical-based cathode, by using the increased free radical density polymer (PDDP) as the cathode material for a higher specific capacity Li-ion battery. Also, the electrochemical properties and the charge–discharge mechanism of the prepared polymer during the charge–discharge process were systematically investigated.

2. Experimental

Material synthesis

Material. Diphenylamine (98%), 1,4-dibromobenzene (99%), triphenylamine (98%), tri-*tert*-butylphosphine ($PtBu_3$, 1.0 M), sodium *tert*-butoxide (NaO^tBu, 98%), and palladium acetate ($Pd(OAc)_2$, AR) were purchased from Energy Chemical Reagent Co. All other reagents were received as analytical grade and used without further purification.

Synthesis of DDP monomer. *N*,*N*,*N*,*N*-tetraphenylphenylenediamine (DDP) was synthesized according to the ref. 20: 0.020 mol diphenylamine, 0.010 mol 1,4-dibromobenzene and 0.020 mol NaO^tBu were dissolved in 40 mL toluene, to which 0.1 g $Pd(OAc)_2$ and 3 mL $PtBu_3$ were added. The mixture was stirred in an Ar atmosphere at 110 °C for 12 h. The final solution was extracted with CH_2Cl_2 and water. Then, CH_2Cl_2 was removed by rotary evaporation to afford the crude product, which was purified by column chromatography on silica gel with petrol ether as the eluent. The product was obtained as a white crystal in an 88.5% yield. MS (EI): calculated for $C_{30}H_{24}N_2$ *m*/*z*: 412.5, found *m*/*z*: 412.5.

Chemical polymerization of PTPA and PDDP. The polymers of poly(*N*,*N*,*N*,*N*-tetraphenylphenylenediamine) (PDDP) and poly(triphenylamine) (PTPA) were prepared by chemical oxidative polymerization in chloroform (20 mL) using ferric chloride as the oxidant. The solution was stirred overnight at room temperature under N_2. After completion of the solution polymerization reaction, the reaction mixture was poured into methanol to deposit the polymer product, which was then filtered and washed with methanol several times. Finally, the polymer product was filtered and dried in vacuum at 60 °C for 12 h. The colors of the PTPA and PDDP were yellow and green, respectively. Pyrolysis-gas chromatography chromatography-mass spectrometry (PTPA): retention time (31.86 min), molecular weight (245.10), pyrolysis-gas chromatography-mass spectrometry (PDDP): retention time (55.03 min), molecular weight (412.26).

Material characterization

Pyrolysis-gas chromatography-mass spectrometry (Py-GC) was carried out on a vertical microfurnace pyrolyzer (PY2020iD, Frontier Lab Ltd, Fukushima, Japan), which was directly attached to a gas chromatograph (CP-3800, Varian, USA) equipped with a flame ionization detector (FID). Raman spectra were recorded on a Lab RAM HR UV800 (JOBIN YVON, France). UV-Vis spectra were recorded on a Varian Cary 100 UV-Vis spectrophotometer (Varian, USA). The electron spin resonance (ESR) spectra were recorded on a BRUKER A300 spectrometer (Switzerland). Scanning electron microscopy (SEM) measurements were taken using a Hitachi S-4800 scanning electron microscope (Hitachi, Japan). The cyclic voltammograms (CV) tests were performed with a CHI 660C electrochemical working station in 0.1 M $LiClO_4/CH_3CN$ *versus* Ag/AgCl at a scan rate of 10 mV s^{-1}. Spectroscopy (EIS) experiments were carried out at an open circuit voltage (OCV) of frequency ranges from 0.1 Hz–1 MHz in a CHI 660C electrochemical working station by the assembled stimulant lithium ion half-cells.

Electrochemical measurements

For cathode characterization, a CR2032 coin-type cell was used, which was assembled in an argon-filled glove box. The cathode electrodes were prepared by coating a mixture containing 50% of the prepared polymers, 40% acetylene black, and 10% PVDF binder on circular Al current collector foils, followed by drying at 60 °C for 24 h. Afterward, the cells were assembled with lithium foil as the anode, the prepared electrodes as the cathode, and 1 M LiPF6 dissolved in ethylene carbonate (EC) and dimethyl carbonate (DMC) (EC/DMC = 1 : 1 v/v) as the electrolyte. The charge–discharge measurements were carried out on a LAND CT2001, using a constant current density at room temperature.

3. Results and discussion

Material characterization

RS. Fig. 1 shows the Resonance Raman spectra of the as-prepared PTPA and PDDP. The main characteristic peaks of the

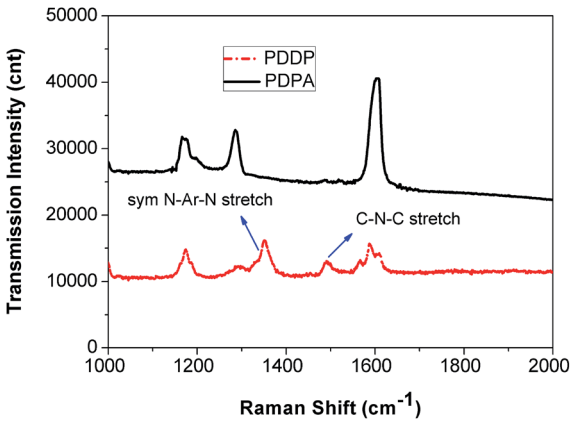

Fig. 1 Resonance Raman spectra of the PTPA and PDDP samples measured at 632.81 nm.

triphenylamine moieties have been displayed in the two samples, which are assigned as follows: 1167 cm^{-1} (C–H in-plane stretching), 1287 cm^{-1} (C–C inter-ring stretching), 1489 cm^{-1} (C=N stretching), and 1606 cm^{-1} (C–C ring stretching).[21–23] In contrast to PTPA, a new band at 1350 cm^{-1} appears in the spectrum of PDDP, which is attributed to the symmetric N–Ar–N stretching. These indicate that the *p*-phenylene moieties have been successfully contained in the PDDP polymer, but are absent from PTPA.

ESR. Electron spin resonance was employed to further confirm the existence of radicals in the products of PTPA and PDDP (Fig. 2). As can be seen, a small and broad peak (*g* value: 2.00654) is observed in the spectrum of PTPA, corresponding to the existence of free radicals in the triphenylamine moieties of PTPA. In comparison, the free radical characteristic peak (*g* value: 2.00475) for PDDP becomes broad, with an obvious enhanced intensity, which can be attributed to the specific molecular structure of PDDP with the higher free radical density.[24]

UV-Vis. UV-Vis spectra (normalized absorbance) are very useful for exploring the electro-structure of materials and here were utilized to explore the characteristics of the monomers (TPA and DDP) and the corresponding polymers (PTPA and PDDP). As depicted in Fig. 3, the TPA monomer exhibits one pair of absorption peaks at 305 nm, which are assigned to the π–π* electron transition from the triphenylamine units. In comparison, the π–π* electron transition of DDP monomer red-shifts to 338 nm, due to the extensional π–π* conjugated structure of DDP. After the chemical polymerization, it can be seen that the corresponding absorption peaks of the π–π* electron transition for the obtained PTPA and PDDP become further red-shifted in comparison with that of the TPA and DDP monomers, which can be attributed to the expansion of the π-conjugated systems by the produced conjugated polymer system.[25,26] Still, the absorption peak of PDDP shifts to 390 nm, which is obviously larger than that of PDPA (356 nm). This indicates, due to the higher radical density structure in the repeating unit of PDDP, that the charge carrier transportation alone in the polymer main chain of PDDP is even smoother than that of PDPA.

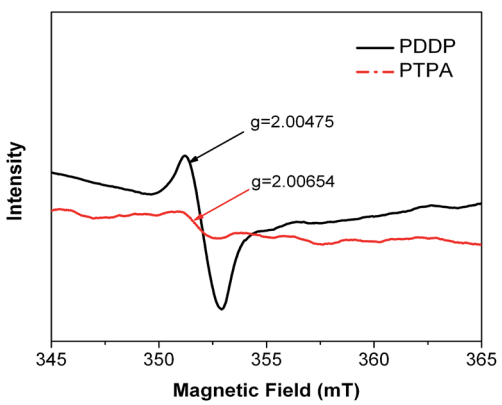

Fig. 2 ESR of PTPA and PDDP measured in the power state.

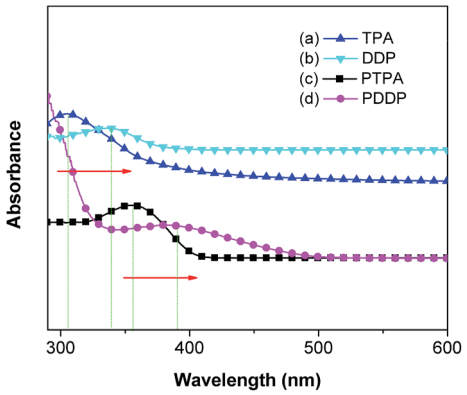

Fig. 3 UV-Vis spectra of (a) TPA, (b) DDP, (c) PTPA, and (d) PDDP (10^{-3} g L^{-1}) in DMF.

SEM. The morphologies of PTPA and PDDP are also shown in Fig. 4. The PTPA polymer presents a serious aggregation structure with the size of several micrometres (Fig. 4a and c). The steric torsion nature of the main chains by the big triphenylamine units may be responsible for this structural feature. However, the morphology of PDDP is different from that of PTPA under the same experimental conditions. As shown in Fig. 4b and d, PDDP exhibits a regularly spherical structure assembled by many small particles of about 500 nm with good dispersion. The different morphologies can be attributed to the different molecular structures of PDDP and PDPA, which have an effect on the molecular aggregation behaviour, as well the resulting morphologies of the polymers. This uniform microstructural feature of PDDP will favor both electrolyte diffusion and the lithium ionic migration in the polymeric electrode, benefiting the improvement of the electrochemical properties during the charge–discharge reaction.

Electrochemical performance

Fig. 5 shows the cyclic voltammetry (CV) profile of PTPA and PDDP measured in 0.1 M lithium perchlorate/acetonitrile solution. The electrode of PTPA exhibits a couple of anodic and

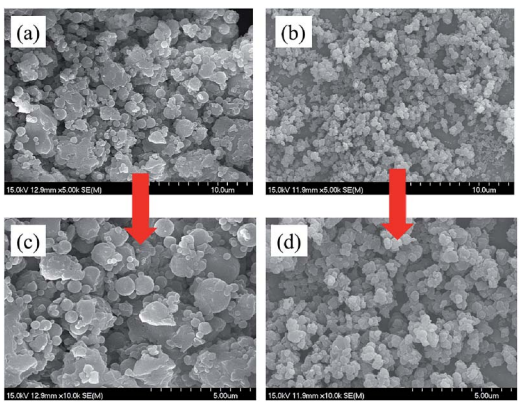

Fig. 4 SEM images of powder samples (a) PTPA, (b) PDDP, (c) and (d) partially enlarged SEM image in (a) and (b), respectively.

cathodic peaks at about 1.05 V and 0.8 V, respectively. The potential separation between the oxidation and reduction peaks is about 0.25 V, and the approximately symmetrical peaks suggests a good insertion/extraction reversibility of the produced PTPA. Comparably, there are some obvious differences for the CV curves of PDDP, in which it displays two pairs of redox peaks, corresponding to the characteristics of both the free radical centers for the DDP moieties of PDDP. Therein, one pair of redox peaks located at 0.60 (reduction) and 0.82 V (oxidation) is attributed to the first radical cation reaction during the p-type doping process, which is obviously below the redox peaks of PTPA.[27] The other couple of redox peaks at high potential (1.32 and 1.08 V) can be assigned to the formation of the second cation radical. Furthermore, two pairs of anodic and cathodic peaks in PDDP still keep the approximately symmetrical peaks and almost equal peak areas, suggesting good insertion/extraction reversibility for the advanced electrode material during the charge–discharge process.

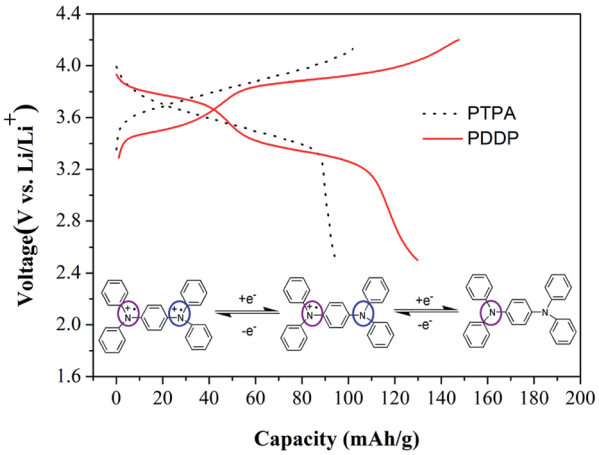

Fig. 6 Initial charge–discharge profiles of PTPA and PDDP electrode material at a constant current of 20 mA g^{-1} between 2.5 and 4.2 V [inset: the possible charge–discharge process of PTPA and PDDP].

Charge–discharge performance

The charge–discharge behaviors of the as-prepared polymers as cathodes of lithium batteries were systematically investigated by the simulated lithium ion half-cell method. As shown in Fig. 6, PTPA shows an initial discharge capacity of 94.7 mA h g^{-1}, with a typical voltage plateau in the voltage range of 3.5–4.1 V at the initial cycle, corresponding to the report.[14] In comparison, under the same conditions, the PDDP electrode exhibits an initial discharge capacity of up to 129.1 mA h g^{-1}, which is higher than that of the measured and reported PTPA, with two obvious voltage platforms at about 3.8 and 3.3 V, respectively, in accord with the redox couples observed in the CV analysis (Fig. 5). Therein, the high voltage plateau in the voltage range of 3.4–4.2 V is attributed to the higher redox couple, which provides a discharge capacity of about 62.5 mA h g^{-1}, while the other lower plateau in the voltage range of 2.5–3.4 V corresponds to the lower redox couple, which has a discharge capacity of about 67.5 mA h g^{-1}. The almost identical discharge capacity for the two stage discharge processes indicates that both free radicals in the DDP moieties perform the same action, which is consistent with the symmetrical peak area of the two pairs of redox couples (as shown in the CV analysis of PDDP). It is reasonable to assume that the redox characteristics of PDDP are exhibited in a one-by-one two stage redox reaction. The improved capacity can be attributed to the higher free radical density, as well the resulting high theoretical capacities of PDDP. Furthermore, the tiny and uniform particle morphology of PDDP compared to that of PTPA further facilitates the diffusion of the electrolyte solution to the active-polymer center and the improvement of the PDDP performance to some degree (as shown in Fig. 4b).

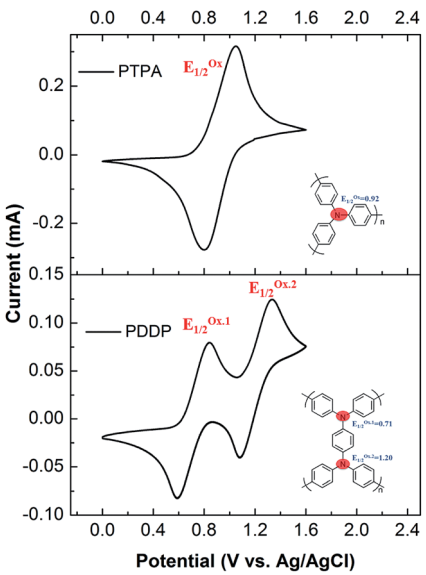

Fig. 5 Cyclic voltammograms (CV) of PTPA and PDDP in 0.1 M $LiClO_4$/CH_3CN *versus* Ag/AgCl at a scan rate of 10 mV s^{-1} [inset: the possible oxidation order of the redox centers of PTPA and PDDP].

The possible reason for the two symmetrical discharge voltage plateaus displayed by PDDP may be that during the first stage discharge process, one of the free radical cation centers functions as an electron-withdrawing group to another free radical cation center in the same DDP moiety, and this electron-withdrawing effect of the first radical cation tunes the HOMO (highest occupied molecular orbital) energy level of the second radical cation, which is closely related to the redox potential.[28] After the first stage of the free radical discharge process, one of free radical cations in the DDP units accepts one electron to become an electron pair, which further acts as an electron donating group to the remaining free radical cation. Due to the electron donating effect of the formed amino-contained group, the SOMO (single occupied molecular orbital) energy level of the last radical cation decreases, leading to the drop of the redox potential during the second stage of the free radical discharge. The related mechanism for this is shown in Fig. 7.

The cycling stability of the as-prepared polymers as cathode materials was also examined, and is shown in Fig. 8. It is found that both the PDDP and PTPA electrodes show a similar cycling

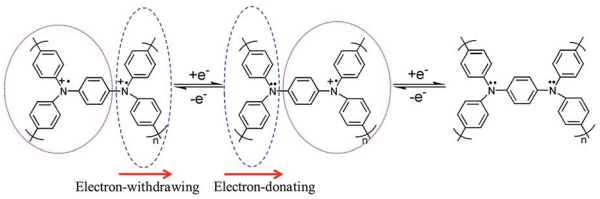

Fig. 7 Schematic diagram of the possible electron donating/withdrawing effect during the two charge–discharge stages.

performance, which is decided by the nature of the organic-based material electrode. In particular, the cycling stability testing of PDDP exhibits a serious capacity degradation in the initial 10 cycles, while the capacity of the following cycles maintains relatively stable. The initial capacity degeneration is possibly caused by the serious re-aggregation of PDDP during the initial 10 charge–discharge cycles, due to the pristine looser stacking micro-structure of PDDP than that of PTPA. Furthermore, it can be seen that although the discharge capacity of PDDP drops from its initial 129.1 mA h g^{-1} to 110.6 mA h g^{-1} after 50 cycles, it is still higher than the initial capacity of PTPA, demonstrating that the PDDP electrode presents excellent electrochemical stability.

The rate performances of the polymer electrodes were further examined at different current rates of 50, 100, 300, and 500 mA g^{-1}, respectively. Compared with the parent PTPA, the PDDP electrodes display an improved rate capability, with an enhanced current rate from 50 to 500 mA g^{-1}, as shown in Fig. 9. The specific capacities for PDDP are 122.4, 118, 104.8, and 92.8 mA g^{-1}, respectively, with a 10-fold increase in the current from 50 to 500 mA g^{-1}, which, though, are still higher than that of PTPA at a high current rate, although the decay rate of the capacity is also comparatively high. In addition, PTPA and PDDP present a quickly recovered capacity ability, as the current rate further returns to 50 mA g^{-1}. The possible reasons for the improved high rate capability can be partly ascribed to the higher radical density structure in the repeating unit of PDDP, which leads to the charge carrier transportation in the polymer main chain of PDDP being even smoother than that of PDPA. In addition, the uniform micro-structural features of PDDP will further benefit the ions (PF^{6-} and Li^{+}) insertion-extraction process during the charge–discharge process, which also causes the high rate capability. Thus, the PDDP polymer would be a good potential candidate for the cathode materials of high-power lithium batteries.

Fig. 10 shows the electrochemical impedance spectra of pristine PTPA and PDDP. The impedance spectra can be explained on the basis of an equivalent circuit with an electrolyte resistance (R_e), charge transfer resistance (R_{ct}), double layer capacitance and passivation film capacitance (CPE), and Warburg impedance (Z_w).[29,30] In these impedance plots, the initial intercept of the spectrum at the Z_{re} axis at high frequency corresponds to the resistance of the electrolyte (R_e). The semicircles at low impedance frequencies represent the charge transfer reaction resistance (R_{ct}), while the straight lines at low frequencies indicate the Warburg impedance(Z_w), which shows

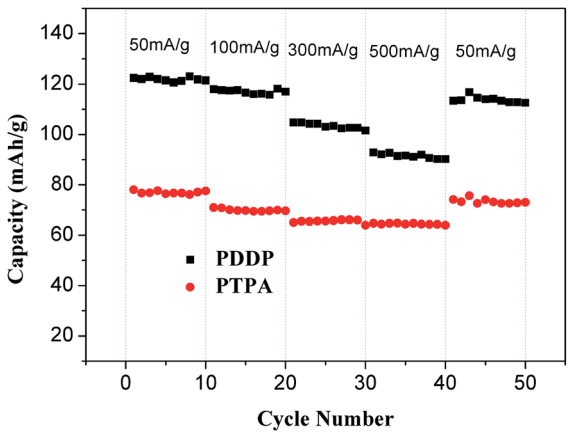

Fig. 9 Rate performances of the polymer electrodes in the voltage range from 2.5–4.2 V at various current rates of 50, 100, 300 and 500 mA g^{-1}.

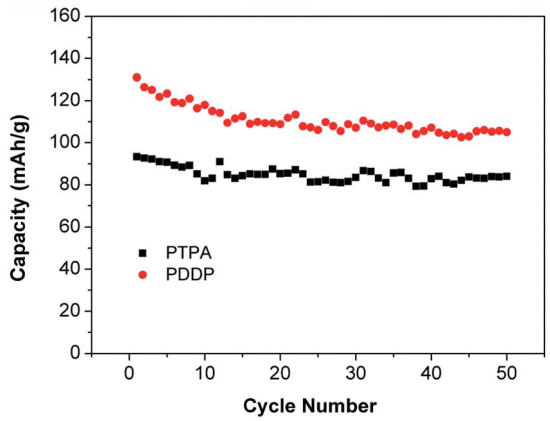

Fig. 8 Cycling stability of the polymer electrodes material at a constant current of 20 mA g^{-1} between 2.5 and 4.2 V in LiPF6 EC/DMC (v/v, 1 : 1) electrolyte *versus* Li/Li^{+}.

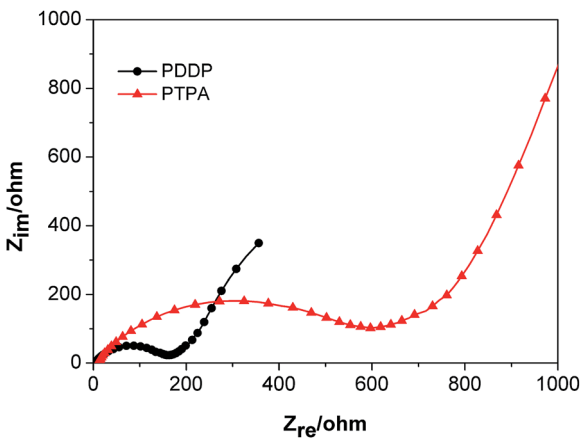

Fig. 10 EIS of PTPA and PDDP samples in the Li/electrolyte/sample configuration.

the diffusion-controlled process. As can be seen in Fig. 10, the R_e is almost the same for the cells with different cathode materials, indicating that there is no significant change in the ionic conductivity of the electrolyte or mobility of the ions with the different cathode-based cells during the cycling process. The charge transfer resistance (R_{ct}) varies with different cathodes: 600 Ω for the PTPA electrode and only 160 Ω for PDDP. And the reduced charge transfer resistance of PDDP may be ascribed to the delicate molecular structures and the high free radical density, which leads to charge migration occurring smoothly along the polymer chain. The smooth charge migration for PDDP compared to PTPA was also proven by the UV-Vis spectra (as displayed in Fig. 3). In addition, the smaller particles and the loose structure of the PDDP will provide a higher specific surface area, making the electrolyte penetration easier during the redox reaction, which also facilitates the decrease of the charge transfer reaction resistance.

4. Conclusions

PDDP with a high free radical density structure has been firstly applied as a cathode material, and has been shown to present two well-defined plateaus, with quite a high capacity of 129.1 mA h g^{-1}. Moreover, the discharge capacity of PDDP retained over 110.6 mA h g^{-1} after 50 cycles, which was still higher than the initial capacity of PTPA. UV-Vis spectra and EIS tests illustrated the smoother charge migration in the PDDP polymer bulk than in that of PTPA, which was attributed to the intensive free radical density structure and the improved morphology of PDDP. The excellent electrochemical performances of PDDP indicated that it was a promising strategy for the design and preparation of a high capacity cathode with a high free radical density structure *via* increasing the number of radicals in the repeating unit.

Acknowledgements

The authors gratefully thank the National Natural Science Foundation of China (NSFC, no. 51003095, no. 51103132) and Research on Public Welfare Technology Application Projects of Zhejiang Province, China (2010C31121) for financial support. This work also was supported by the analysis and testing foundation of Zhejiang University of Technology.

Notes and references

1 V. Etacheri, R. Marom, R. Elazari, G. Salitra and D. Aurbach, *Energy Environ. Sci.*, 2011, **4**, 3243.
2 L. Taberna, S. Mitra, P. Poizot, P. Simon and J. M. Tarascon, *Nat. Mater.*, 2006, **5**, 567.
3 M. Morcrette, P. Rozier, L. Dupont, E. Mugnier, L. Sannier, J. Galy and J. M. Tarascon, *Nat. Mater.*, 2003, **2**, 755.
4 N. Du, H. Zhang, B. D. Chen, J. B. Wu, X. Y. Ma, Z. H. Liu, Y. Q. Zhang, D. R. Yang, X. H. Huang and J. P. Tu, *Adv. Mater.*, 2007, **19**, 4505.
5 P. Novak, K. Müller, S. V. Santhanam and O. Hass, *Chem. Rev.*, 1997, **97**, 207.
6 Z. P. Song, H. Zhan and Y. H. Zhou, *Angew. Chem., Int. Ed.*, 2010, **49**, 8444.
7 N. Oyama, T. Tatsuma, T. Sato and T. Sotomura, *Nature*, 1995, **373**, 598.
8 M. Yao, H. Senoh, S. I. Yamazaki, Z. Siroma, T. Sakai and K. Yasuda, *J. Power Sources*, 2010, **195**, 8336.
9 X. Han, C. Chang, L. Yuan, T. Sun and J. Sun, *Adv. Mater.*, 2007, **19**, 1616.
10 T. L. Gall, K. H. Reiman, M. C. Grossel and J. R. Owen, *J. Power Sources*, 2003, **119–121**, 316.
11 R. H. Zeng, X. P. Li, Y. C. Qiu, W. S. Li, J. Yi, D. S. Lu, C. L. Tan and M. Q. Xu, *Electrochem. Commun.*, 2010, **12**, 253.
12 T. Suga, H. Ohshiro, S. Sugita, K. Qyaizu and H. Nishide, *Adv. Mater.*, 2009, **21**, 1627.
13 K. Qyaizu and H. Nishide, *Adv. Mater.*, 2009, **21**, 2339.
14 U. Mitschke and P. Bauerle, *J. Mater. Chem.*, 2000, **10**, 1471.
15 A. Petr, C. Kvarnstrom, L. Dunsch and A. Ivaska, *Synth. Met.*, 2000, **108**, 245.
16 M. E. Roberts, D. R. Wheeler, B. B. McKenzie and C. B. Bruce, *J. Mater. Chem.*, 2009, **19**, 6977.
17 T. K. Jeremy and E. R. Mark, *J. Mater. Chem.*, 2012, **22**, 25447.
18 J. K. Feng, Y. L. Cao, X. P. Ai and H. X. Yang, *J. Power Sources*, 2008, **177**, 199.
19 U. Mitschke and P. Bauerle, *J. Mater. Chem.*, 2000, **10**, 1471.
20 O. Mi, W. Genghao and Z. Cheng, *Electrochim. Acta*, 2011, **56**, 4645.
21 V. S. Adriana, E. Marco, E. Volker, S. Michael, A. Stephan, K. Volker, N. Gilbert, S. Rainer, L. Christoph, L. Dirk, S. Dietmar and Z. Manfred, *J. Am. Chem. Soc.*, 2004, **126**, 7834.
22 M. Jain and S. Annapoorni, *Synth. Met.*, 2010, **160**, 1727.
23 M. Zhou, K. Wang, Z. W Men, S. Q. Gao, Z. W. Li and C. L. Sun, *Spectrochim. Acta, Part A*, 2012, **97**, 526.
24 C. Junsang, U. Kumiko, Y. Naoki and Y. Kimihisa, *Sci. Technol. Adv. Mater.*, 2004, **5**, 697.
25 S. C. Hsu, W. T. Whang and C. S. Chao, *Thin Solid Films*, 2007, **515**, 6943.
26 H. C. Ko, D. K. Lim, S. H. Kim, W. Choi and H. Lee, *Synth. Met.*, 2004, **144**, 177.
27 W. Huimin and H. Shenghuei, *J. Polym. Sci., Part A: Polym. Chem.*, 2011, **49**, 337.
28 T. Suga, Y. J. Pu, S. Kasatori and H. Nishide, *Macromolecules*, 2007, **40**, 3167.
29 S. Rodrigues, N. Munichandraiah and A. K. Shukla, *J. Solid State Electrochem.*, 1999, **3**, 397.
30 F. Nobili, F. Croce, B. Scrosati and R. Marassi, *Chem. Mater.*, 2001, **13**, 1642.

